INVESTIGATING THE BUCKLING BEHAVIOR OF OSB PANELS

Edmond P. Saliklis
Assistant Professor

and

Amy L. Mussen
Student
Department of Civil and Environmental Engineering
Lafayette College
Easton, PA 18042

(Received December 1998)

ABSTRACT

A fully nonlinear finite element buckling analysis, incorporating geometric and material nonlinearities, was conducted on oriented strandboard (OSB) panels. A much simpler finite element eigenbuckling analysis was also conducted. An interesting intermediate approach was then investigated, that is an eigenbuckling analysis of initially imperfect plates. It was found that the eigenbuckling analysis provided good insight into the physical behavior of the panels and predicted the buckling loads of OSB panels within 20% of the experimentally obtained values, yet required significantly less modeling effort than did the fully nonlinear analysis. We propose this as a practical means of establishing the buckling loads of simply supported OSB panels. A number of issues regarding the initially imperfect shape of the panel were explored and are discussed herein.

Keywords: Oriented strandboard, buckling, eigenbuckling, finite element analysis.

INTRODUCTION

There is a need for validation of simplified finite element eigenbuckling methods to make buckling analysis more readily understandable to engineers and researchers involved in the practical investigation of buckling of wood-based panels. One would not use an eigenbuckling analysis as a final prediction of column buckling, nor for the buckling of cylindrical shells since such results are often grossly unconservative. Yet we were surprised to find that the eigenbuckling predictions for the buckling loads of oriented strandboard panels were quite satisfactory. To check the validity of our eigenbuckling results, we compared them to experimentally obtained data, as well as to a fully nonlinear finite element prediction of the buckling loads. During the course of this investigation, it was noted that the initial geometric imperfections played a major role in the nonlinear finite element predictions, as was expected. What we did not anticipate was the effect of the initial imperfections in the numerical eigenbuckling analysis. The results of this part of the study will be presented, yet we have not explored the mathematics of imperfect panel eigenbuckling. We will continue work on this area in the future.

The buckling load of oriented strandboard (OSB) panels is difficult to predict for a number of reasons. First, the material itself is not homogeneous. The nonhomogeneity of the material has been modeled (Kamiya and Itani 1998) as an orthotropic solid with three mutually perpendicular planes of elastic symmetry. Another modeling challenge arises from the fact that OSB exhibits nonlinear load vs. deformation behavior (the constitutive relationship). This nonlinearity on each orthotropic axis must be addressed carefully, so as to not violate fundamental mechanical principles, although in practice, OSB is traditionally modeled as having a linear constitutive relationship on each principal plane.

Wood and Fiber Science, 32(3), 2000, pp. 259–268

The calculation of buckling loads can be important in the growing use of OSB as seismic horizontal diaphragm. Diaphragms in seismic design receive load in the plane of the panel; thus buckling loads could become a design concern (Lindeburg 1998). However, research has shown (Karacabeyli and Ceccotti 1998) that nailing schedules and other construction practices may well have a substantial influence on the structural performance during a seismic event. The experimental data we gathered here in this study are preliminary, yet the trends captured in these tests are quite interesting.

Very little research has been reported in this area. Perturbation techniques have been used (Shen 1995) to study the generalized buckling behavior of orthotropic plates. Others have used asymptotic techniques (Zhang and Shen 1991) and have included the use of imposing initial geometrical imperfections. These researchers found that for orthotropic plates, the buckling mode shape was affected by the orthotropicity of the panel (ratio of E_{strong}/E_{weak}, where E is the modulus of elasticity). Zhang and Shen found that the buckling loads were somewhat affected by the magnitude of initial imperfections. These insights were interesting to us and prompted us to see whether or not similar effects of imperfections could be found in an eigenbuckling procedure. Some researchers (Hahn et al. 1992; Easley 1975) have reported experimental buckling setups. Hahn et al. took extreme care to ensure that individual points along the supported edges could rotate independently of one another. We attempted to recreate such "true pinned" connections on a smaller prototype device, but rejected it in our final buckling device on the basis of cost and simplicity. While the experimental devices proposed by Hahn and Easley may achieve their proposed goals, the details look complicated and difficult to reproduce from the few photographs provided. To the authors' knowledge, no studies of the buckling of OSB using experimental data and finite element procedures have been reported. Here at Lafayette College, we have embarked on a number of closed-form and numerical investigations of OSB response. The objective of this study was to examine whether or not an eigenbuckling analysis would give satisfactory results for the prediction of buckling loads of OSB panels.

EXPERIMENTAL METHODS

Material property tests

Static tests were performed on one thickness of OSB panels, 11.1mm (7/16 in.) thick, purchased commercially to obtain fundamental material properties. Two types of static tests were conducted-strip bending and plate twisting. Strip bending nearly conformed to ASTM D3043 Method B (ASTM 1997) and was used to extract the material property E_i, the modulus of elasticity (MOE). Method B was chosen since we were interested only in the initial modulus of elasticity along each principal orthotropic axis (E_{strong} and E_{weak}); we did not seek the modulus of rupture. The new experimental device did not have the roller/bearing system proposed by standard D3043 to eliminate torsional restraint, but it did meet all of the demands of the radius of curvature of the supporting rollers. Bending specimens of 50.8-mm width (2 in.) were used, in the MOE tests. Standard D3043 (ASTM 1997) recommends either 50.8-mm (2-in.)-wide or 304.8-mm (12-in.)-wide specimens. Clearly, the material's nonhomogeneity would have required us to use the 304.8-mm-wide specimens if we sought the modulus of rupture, as pointed out by McNatt et al. (1990). McNatt also points out that some researchers found no variation of MOE calculated for plywood and waferboard based on specimen width, whereas others found a 10% to 20% reduction of MOE calculated from narrower specimens (McNatt et al. 1990). For the sake of completeness, we have calculated the eigenbuckling values of OSB panels based on our apparent MOE readings ($E_{apparent}$) from the 50.8-mm-wide specimens, as well as the purported true reading increased by 15% ($E_{adjusted}$) as suggested by McNatt et al. (1990). This provided the addi-

TABLE 1. *Summary of input material properties.*

E strong apparent MPa	E weak apparent MPa	E strong adjusted MPa	E weak adjusted MPa	G no adjustment MPa	Moisture content 8.4% to 9.60%
4,262	1,899	4,900	2,184	1,560	

tional benefit of quantifying the sensitivity of the buckling load to variations in the MOE. All specimens were preconditioned in a humidity-controlled environment prior to testing. The temperature in the room ranged between 70° and 75° F, while the relative humidity was controlled to remain at 66% ± 7% again, not quite to ASTM standards, but this was the level of control we were able to attain. Such preconditioning resulted in specimen moisture content between 8.5% and 9.5%.

We performed simplified ultimate stress tests on small machined specimens of OSB, using the "Alternative Test for Evaluation of Maximum Compressive Strength Only" from ASTM Standard D3501 (ASTM 1997). We found the following axial ultimate compressive stresses by this technique, and took the shear ultimate stress from the literature (PFS 1997): σ_{strong} = 13.1 MPa (1900 psi), σ_{weak} = 8.4 MPa (1216 psi), and τ_{ult} = 7.6 MPa (1100 psi). We verified our ultimate compressive strength numbers with those obtained in a commercial laboratory (Shrestha 1999).

The plate twisting conformed to ASTM D 3044 (ASTM 1997) and 609.6-mm (24-in.) square specimens are used. These specimens were also humidity-preconditioned. This test determined the material property G_{ij}, the in-plane shear modulus. The in-plane shear modulus is the modulus that affects panel buckling (ASTM 1997). Since the shear testing specimens were considered large, with respect to flake size, we saw no need to adjust the obtained shear modulus. However, we did investigate how sensitive the buckling results are to variations in G_{ij}. We found that a 15% variation in G_{ij} results in a 6% variation of the eigenbuckling load. Table 1 summarizes the initial MOE used in this study, labeled as apparent moduli, and then the second set of moduli labeled as adjusted moduli, these are 15% larger than the apparent moduli. The eigenbuckling computer models were conducted using both sets of moduli to quantify sensitivity to MOE inaccuracies.

Buckling tests

Buckling tests were conducted to capture the unique relationship of material properties coupled with specimen geometry that result in an instability load (the buckling load). Buckling tests were performed on rectangular specimens with simply supported boundary conditions on all four edges of the panel. We simulated a simply supported boundary condition to recreate the effect of a nailed panel edge. While experimental work conducted by Karacabeyli and Ceccotti (1998) on seismic loading of wood-frame shear walls clearly shows several failure modes of the nails themselves, such investigations of nail failures were beyond the scope of this research. We concentrated solely on the mechanics of the panels themselves. Panel width was limited to 304.8 mm (12 in.), while panel length was either 609.6 mm (24 in.) or 914.4 mm (36 in.). The 305-mm to 914-mm panel breadths were chosen to encompass spans that might be encountered in actual joist spacings, typically on the order of 406 mm (16 in.). In all, 49 panels were tested to failure (28 loaded along the strong axis and 21 loaded along the weak axis). The determination of the buckling load was simple for the cases of sudden, catastrophic failures. In other cases, however, a measured lateral deflection on the order of the panel thickness constituted failure. The 304.8-mm by 914.4-mm (12-in. by 36-in.) panels loaded along the strong principal axis will be referred to as A_Strong. Other panel configu-

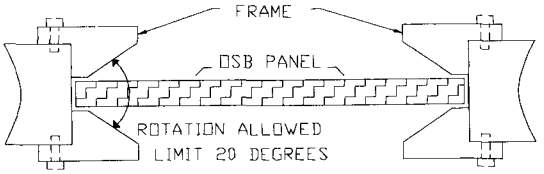

FIG. 1. Plan view of buckling device.

rations become apparent using this nomenclature; 304.8 mm by 914.4 mm loaded in the weak direction is A_Weak, and 304.8 mm by 609.6 mm (12 in. by 24 in.) loaded in the strong direction is B_Strong and then B_Weak.

Figures 1 and 2 show the buckling device and the end conditions of the panel. The simply supported boundary conditions were achieved here by allowing the panel to rotate a finite amount, here 20° without translating. Load is applied along one axis, (either strong or weak) and all four edges were simply supported. We observed that during the application of load, the central portion of the panel often tended to bulge out more than other portions, (a Mode 1 half sine wave buckling shape), yet in other instances one portion may have bulged forward and the other backward (a Mode 2 full sine wave buckling shape). In general, the longer panels (A_Strong and A_Weak) tended to buckle in a Mode 2 full sine wave shape, whereas the shorter panels tended to buckle into a Mode 1 Shape. Details of all these experimental setups can be found in Saliklis (1999).

Numerically predicting the buckling load via eigenbuckling

The finite element method was used in several different ways to predict the buckling load. First, an eigenbuckling analysis was performed on initially flat plates, simply supported on all four sides. This was the impetus of the study, to determine whether or not such a simplified finite element analysis is accurate in determining buckling loads. A curious insight was noted during these analyses, that the eigenbuckling problem gives slightly different results if the plate is initially imperfect. We postulate that the stiffness matrix is reformu-

FIG. 2. Buckling device with specimen.

lated to take into account the panel curvature in such a case. We did not explore this further, other than to report the results as a second eigenbuckling analysis, done on initially imperfect plates. Finally, a nonlinear buckling analysis was performed on initially imperfect plates.

An eigenbuckling analysis is the traditional seeking out of the bifurcation load, i.e., the load at which two solutions (stable and unstable) momentarily converge. Within the context of a finite element analysis, the eigenbuckling analysis is an easy-to-use method. However, it generally gives unconservative results because it can predict a buckling load that is much greater than the actual, experimentally obtained buckling load. It is to be noted that in this analysis, the eigenbuckling analysis gave fairly accurate results, perhaps due to the simply supported boundary conditions on all four sides of the panel and the lack of significant deviations in specimen geometry.

The first eigenbuckling analysis was conducted on initially flat plates, simply supported on all four sides. All four combinations of panel geometry were analyzed, A_Strong, A_Weak, B_Strong, and B_Weak. The eigenbuckling analysis gave the bifurcation load (the buckling load) for various modes, or deformed shapes. To picture this more clearly, take the example of a pin ended column—the lowest eigenbuckling mode would be single curvature (or one half of a sine wave). The next higher mode would be double curvature (a complete sine wave from end to end). Clearly, designers would be interested in only the lowest buckling load; but insights were gained from looking at the first two modes of plate buckling. In all cases, except for A_Strong, the first mode (i.e., single curvature) gave the lowest buckling load. The fact that the eigenbuckling analysis gave preference to a double curvature buckling mode for the A_Strong panels prompted further investigations. The displacement plot of such a full sine wave shape is shown in Fig. 3. Note that isotropic rectangular panels tend to buckle into square folds; thus an isotropic 304.8-mm by 914.4-mm (12-in. by 36-in.) panel would prefer to buckle into triple curvature, with 304-mm (12-in.) waves. The fact that A_Strong preferred a double curvature as its lowest mode shows the influence of the orthotropic material properties.

These insights led to an eigenbuckling analysis of initially imperfect panels. This second analysis took panels that had a small initial imperfection, essentially forming an extremely shallow shell. We investigated several shapes of initial imperfection, and chose the shape shown in Fig. 4 because it did not predispose the lowest buckling load into a single curvature mode shape. We used this same initially imperfect shape in the nonlinear buckling analysis described below. The bifurcation loads were then found for this initially imperfect (shallow shell) plate. The magnitude of the imperfection was 1.25 mm. This resulted in a ratio of imperfection-to-longest panel dimension of approximately 1/1,000. It is interesting to note that these second eigenbuckling results (for initially imperfect plates) gave slightly different, (and in fact improved) results compared to the first eigenbuckling analysis. As in the initially flat plate eigenbuckling analysis, the lowest buckling loads were always for a single curvature mode of failure, except for the 304.8-mm by 914.4-mm (12-in. by 36-in.) panel loaded along the strong axis (A_Strong). The deformations of A_Strong due to an eigenbuckling analysis are shown in Fig. 3. Results are summarized in Tables 2 and 3. As stated in the introduction, each analysis was run with two sets of initial elastic moduli to detect how sensitive our analyses were to changes in the MOE, and to reflect the concern of using narrow strips for the MOE calculations. An encouraging conclusion is that the eigenbuckling analysis performed on flat plates is sufficiently accurate, in that it provides a design engineer with a very reasonable estimation of the buckling load. Furthermore, a 15% variation in MOE produced an 8% to 11% variation in the buckling results in the flat panel eigenbuckling study, showing that the buckling results are also sensitive to the

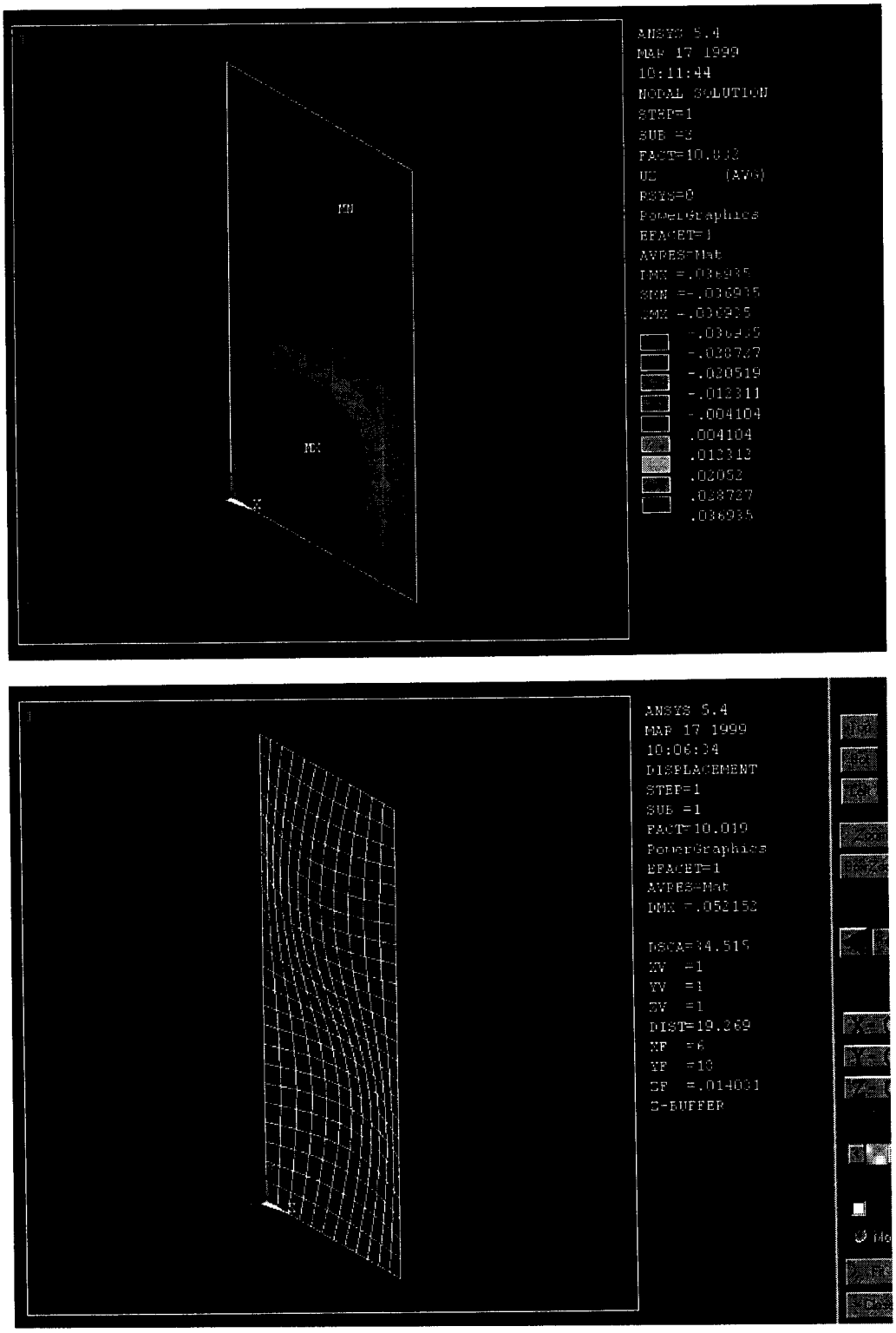

FIG. 3. Plot of finite element results, deformed shape, full sine wave top to bottom.

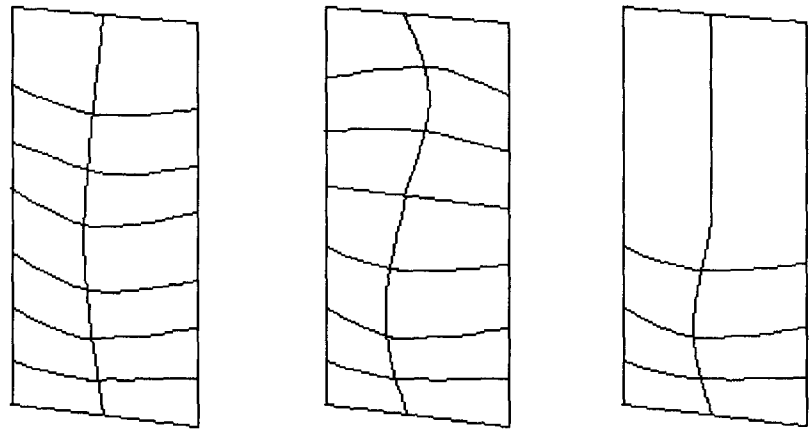

Plate Mode 1 Buckling Eigenbuckling | Plate Mode 2 Buckling Eigenbuckling | Initially Imperfect Shape for Nonlinear Analysis and for Eigenbuckling Analysis

FIG. 4. Mode shapes and shape of initial imperfection.

panel geometry and boundary conditions. This is advantageous because the MOE is not always known with precision. As stated previously, a ±15% variation in G_{ij} produced a corresponding ±6% difference in the eigenbuckling load.

Nonlinear buckling analysis

The nonlinear buckling analysis was the most numerically intensive analysis conducted, and it provided the best correlation to experimental data. In this analysis, large displacements were allowed requiring updates of the current position of the panel at each increment of the analysis. Nonlinear material properties were used in this analysis, whereas the eigenbuckling analysis required only linear elastic data on the constitutive relationship. This modeling refinement must accurately reflect experimental data, yet not violate fundamental thermodynamic principles (Shih and Lee 1978). In the finite element program, the nonlinear buckling option utilized nonlinear constitutive behavior. However, the only nonlinear model available for orthotropic materials was the bilinear model; thus a bilinear curve in each of the three orthogonal directions was used. The first portion of the bilinear curve represented the initially elastic modulus along the axis (strong or weak). The second portion of the bilinear curve can have a second, smaller modulus, or it can have a theoretical zero slope, and would as such be called an elastic-plastic model. The transition point between the two parts of the curve also has a physical significance; it is the yield stress. The data we gathered showed that the material remained linear up till approximately 95% of failure. Therefore, we set the yield stress to be 95% of the ultimate stress. Since we were not interested in the post-buckling response of the

TABLE 2. *Eigenbuckling analysis of initially flat plates, numerically obtained buckling loads.*

A_Strong	E apparent	E adjusted
	44 KN (9,960 lbs)	48 KN (10,806 lbs)
A_Weak	E apparent	E adjusted
	35 KN (7,822 lbs)	39 KN (8,869 lbs)
B_Strong	E apparent	E adjusted
	45 KN (10,056 lbs)	49 KN (11,017 lbs)
B_Weak	E apparent	E adjusted
	36 KN (8,062 lbs)	40 KN (9,039 lbs)

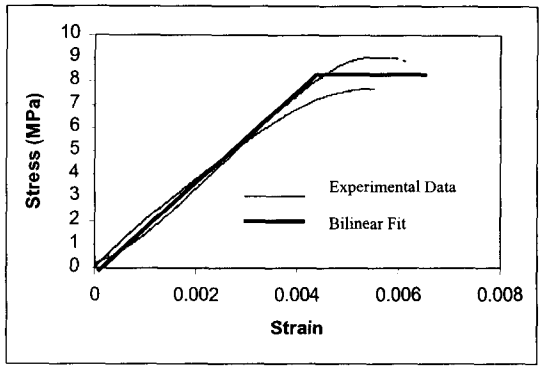

FIG. 5. Bilinear stress vs. strain curves.

panel, it was decided to use the simplest such model, the elastic-plastic model. This required experimental verification of the ultimate stress in each direction, as was done by the methods described in "Material Property Tests" above. Figure 5 shows the constitutive relationships used in this nonlinear analysis for the weak axis. Similar results were found for the strong axis compression data as well as the shear response data. The compression data and the shear data exhibited similar constitutive behaviors insofar as failure occurred soon after this yield stress was reached. We designated the yield stress to be 85% of the ultimate stress for E_{strong}, E_{weak} and for G. As evidenced by Fig. 5, such an elastic-plastic model can fit experimental OSB data.

These parameters were entered into the commercially available finite element program ANSYS. Eight-noded isoparametric shell elements were used to model the OSB panels. Results from early test runs showed a 25.4-mm (1-in.) mesh size to be satisfactory for our work. The panel in the nonlinear buckling computer model was initially imperfect and it was noted that the shape of the initial imperfection strongly influenced the results. Such an influence of initial geometric imperfections has been noted by other researchers as well, albeit less dramatically (Zhang and Shen 1991). Various imperfect shapes were tried, and it was noted that starting with a flat panel for the top specimen half and one half sine wave for the bottom half of the specimen (see Fig. 4) slightly improved the buckling predictions for three out of four loading cases. (see Table 4). Another argument justifying such an initial shape was that the eigenbuckling analysis showed only a small distinction between preferred final buckled shapes (either single curvature or double curvature). Using the geometry of Fig. 4 as a starting configuration did not fully predispose the panel into one configuration or the other; thus it was deemed the most judicious initial shape. Finally, we wanted to compare eigenbuckling results to the nonlinear analysis results using the same initially imperfect shape.

During the nonlinear buckling analysis, loads were applied incrementally. As the stresses gradually increased, each element was checked to see if the yield stress had been reached. If so, the incremental change in stiffness for that element was zero, since the elastic-plastic constitutive relationship was being used. In other words, the tangent stiffness for that element became zero and that element's stress level remained at the yield stress. Panel geometry was continuously updated throughout the analysis. At some point, the equations of equilibrium could no longer be satisfied, this was taken as the buckling load. There was one buckling load for each panel geometry, material property combination.

RESULTS AND COMPARISONS

The experimental buckling loads and the predicted buckling loads agreed within 20% for the four various loading cases that we examined. This was the primary information sought. Additional verification of truly capturing material behavior came from comparing the out-of-plane displacements throughout the tests.

To clarify the relationship between the experimental data and the three buckling analyses performed, Table 4 summarizes all of the findings. Only the lowest (first) buckling loads are reported from the eigenbuckling analyses. As discussed previously, this always took the form of single curvature, except for the case

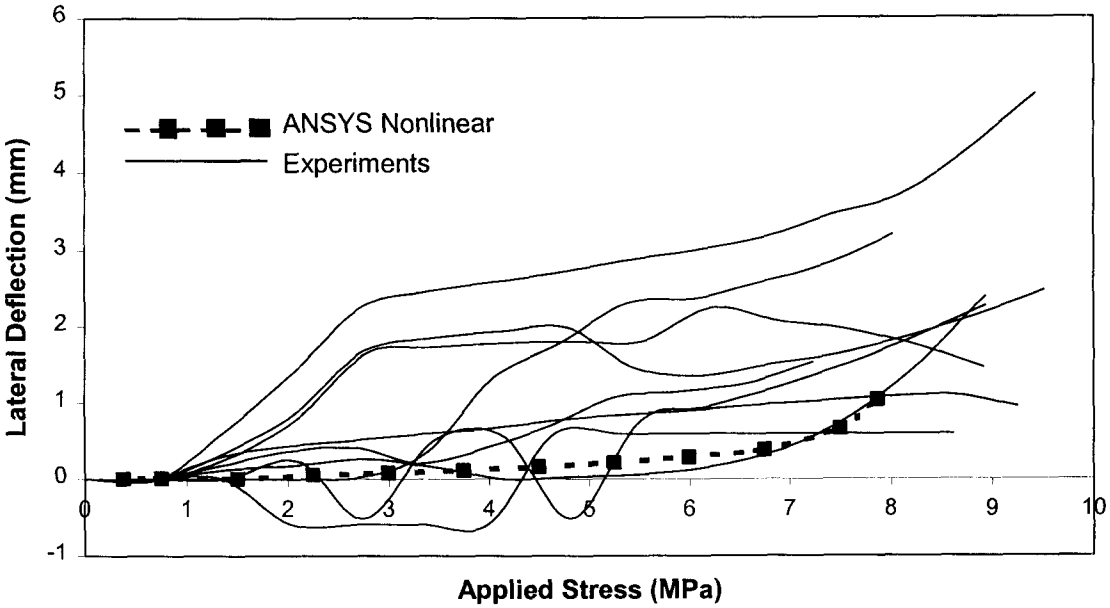

FIG. 6. Typical out-of-plane displacement (B_Weak center node).

of A_Strong. Looking at the data presented in Table 4, one can see that the nonlinear finite element model captured the buckling load within a 7% agreement to experimental data, except for the case of A_Strong. Furthermore, trends that were not captured by the eigenbuckling analyses were better predicted by the fully nonlinear model—for instance, the greatly decreased buckling load going from panels loaded along the strong direction to panels loaded in the weak direction (B_Strong to B_Weak for instance). The imperfect panel eigenbuckling analysis predicted a 14% drop in the buckling load (B_Strong to B_Weak), whereas the nonlinear model was able to predict this decreased buckling load as a 32% decrease, which more accurately reflects the 28% experimental difference.

However, another interesting observation can be drawn from these data when coupled with the numerical modeling effort involved in obtaining these numbers. The nonlinear model does show a 5% to 10% improvement over the eigenbuckling results, but the computational time required to perform a nonlinear buckling analysis far exceeds the time needed to acquire eigenbuckling results. We do not recommend that nonlinear buckling analyses be undertaken; rather, we propose that an eigenbuckling analysis be used for designers and researchers who want to obtain an approximate (within 20%) buckling load.

The sensitivity study of variation of MOE was insightful. First of all, it showed that our apparent moduli readings were in fact adequate, since the artificially adjusted moduli gave less accurate predictions. Secondly, a 15% variation in MOE changed the buckling load only about 8%, which is helpful to know, because there will always be uncertainty in MOE calculations, yet such MOE variations

TABLE 3. *Eigenbuckling analysis of initially imperfect plates, numerically obtained buckling loads.*

A_Strong	E apparent	E adjusted
	44 KN (9,855 lbs)	48 KN (10,703 lbs)
A_Weak	E apparent	E adjusted
	34 KN (7,551 lbs)	38 KN (8,568 lbs)
B_Strong	E apparent	E adjusted
	43 KN (9,694 lbs)	47 KN (10,651 lbs)
B_Weak	E apparent	E adjusted
	37 KN (8,338 lbs)	42 KN (9,342 lbs)

TABLE 4. *Summary of buckling loads, finite element results with apparent moduli. (% error compared to experimental buckling load.)*

Panel	Experimental KN	Number of trials	Stnd. dev. KN	Eigenbck. flat plates KN	Eigenbck. imp. plates KN	ANSYS nonlinear KN
A_Strong	37	8	6	44 (19%)	44 (19%)	43 (16%)
A_Weak	29	20	5	35 (21%)	34 (17%)	30 (3%)
B_Strong	43	11	7	45 (5%)	44 (2%)	42 (−2%)
B_Weak	31	10	2	36 (16%)	37 (19%)	29 (−6%)

did not correspond one-to-one with buckling load predictions. The panel geometry also played a significant role in the calculation of the final buckling load.

The out-of-plane displacements throughout the test were monitored experimentally with displacement transducers. This movement can be compared to the out-of-plane displacements of the nonlinear finite element model. Though this information is not as critical as that provided in Table 4, it does verify the fact that we were accurately modeling material behavior. Figure 6 shows experimental out-of-plane displacement at the location of the displacement transducer, compared with the finite element prediction of out-of-plane movement at that point.

CONCLUSIONS

This study showed that a finite element eigenbuckling analysis gave good insight into the fundamental buckling behavior of simply supported OSB panels, both in terms of buckling load and buckled mode shapes. We recommend that the eigenbuckling method be applied to initially imperfect panels. A small initial imperfection, on the order of 1/1,000th the longest dimension of the panel, was found to be appropriate. Although this procedure has inherent shortcomings, it is preferred to the nonlinear analysis, which is extremely complicated and numerically intensive. Experimentally obtained buckling loads and out-of-plane movement were used to verify the validity of our methods.

REFERENCES

AMERICAN SOCIETY OF TESTING AND MATERIALS (ASTM). Annual book of ASTM standards. Vol. 04.10 Wood. ASTM, West Conshohocken, PA.

EASLEY, J. T. 1975. Buckling forms for corrugated metal shear diaphragms J. Struct. Div. 110(7):1403–1417.

HAHN, E. K., L. A. CARLSSON, AND B. C. WESTERLIND. 1992. Edge-compression fixture for buckling studies of corrugated board panels. Exp. Mechanics 32(9):252–258.

KAMIYA, F., AND R. Y. ITANI. 1998. Design of wood diaphragms with openings. J. Struct. Eng. 124(7):839–848.

KARACABEYLI, E., AND A. CECCOTTI. 1998. Nailed wood-frame shear walls for seismic loads. Test results and design considerations. Paper Ref. T207-6. Struct. Eng. World Wide 1998. Proc. Structural Engineering World Congress, 19–23 July 1998, San Francisco, CA. Elsevier Science, New York, NY.

LINDEBURG, M. R. 1998. Seismic design of building structures. Professional Publications, Inc., Belmont, CA. Pp. 74–89.

MCNATT, J. D., R. W. WELLWOOD, AND L. BACH. 1990. Relationships between small-specimen and large panel bending tests on structural wood-based panels. Forest Prod. J. 40(9):10–16.

PFS RESEARCH FOUNDATION. 1997. Design values for oriented strandboard. Tech. Bull. No. 104, PFS-RF, 2404 Daniels St., Madison, WI 53704.

SALIKLIS, E. P. 1999. Experimentally obtaining stiffness and buckling loads of oriented strand board panels. Proc. 13th ASCE Engineering Mechanics Div. Conference, 13–16 June 1999, Johns Hopkins Univ, Baltimore, MD. (CD-ROM).

SHI, C. F., AND D. LEE. 1978. Further developments in anisotropic plasticity. J. Eng. Mater. Technol. 100:294–302.

SHEN, H. S. 1995. Postbuckling of orthotropic plates on a two-parameter plastic foundation. J. Eng. Mechanics 121(1):50–56.

SHRESTHA, D. 1999. Shear properties tests of oriented strand board panels. Forest Prod. J. 49(10):41–46.

ZHANG, J. W., AND H. S. SHEN. 1991. Postbuckling of orthotropic plates in biaxial compression. J. Eng. Mechanics 117(5):1158–1170.